

# On-Line Fourier Transform Infrared Detection in Capillary Electrophoresis

Malin K  lhed,<sup>†</sup> Peter Hinsmann,<sup>‡</sup> Peter Svasek,<sup>§</sup> Johannes Frank,<sup>‡</sup> Bo Karlberg,<sup>†</sup> and Bernhard Lendl<sup>\*,‡</sup>

Department of Analytical Chemistry, Stockholm University, SE-106 91 Stockholm, Sweden, Institute of Chemical Technologies and Analytics, Vienna University of Technology, Getreidemarkt 9/164, A-1060 Vienna, Austria, and Institute of Industrial Electronics and Material Science, Vienna University of Technology, Gusshausstrasse 25-29/366, A-1040 Vienna, Austria

**The coupling of Fourier transform infrared (FT-IR) spectroscopy as a new on-line detection principle in capillary electrophoresis (CE) is presented. To overcome the problem of total IR absorption by the fused-silica capillaries that are normally employed in CE separations, a micromachined IR-transparent flow cell was constructed. The cell consists of two IR-transparent CaF<sub>2</sub> plates separated by a polymer coating and a titanium layer producing an IR detection window, 150  $\mu\text{m}$  wide and 2 mm long, with a path length of 15  $\mu\text{m}$ . The IR beam was focused on the detection window using an off-axis parabolic mirror in an optical device (made in-house) attached to an external optical port of the spectrometer. The connections between the fused-silica capillaries and the flow cell were made by a small O-ring of UV-curing epoxy adhesive on the sharply cut ends of the capillaries, allowing the capillaries to be easily replaced. Aqueous solutions comprising mixtures of adenosine, guanosine, and adenosine monophosphate were used to test the system's performance. Conventional on-line UV detection was employed to obtain reference measurements of analytes after the IR detection flow cell. The limit of FT-IR detection for all analytes (in absolute amounts) was in the nano- to picogram range corresponding to concentrations in the low-millimolar range.**

Fourier transform infrared (FT-IR) spectroscopy offers non-destructive, molecule-specific information for almost all analytes and is therefore a desirable analytical tool for the detection and identification of a large array of molecules, ranging from small ions to large biomolecules. However, the universal detection provided by techniques such as FT-IR can turn from an advantage to a disadvantage, if applied to liquid solutions without a prior separation step. This is because the solvent matrix will also absorb, and hence limit the technique's applicability, especially when working with aqueous solutions. Therefore, in several previous attempts to hyphenate FT-IR to high-performance liquid chroma-

tography (HPLC) or flow systems,<sup>1–2</sup> two main approaches have been adopted: off-line detection by solvent elimination, and on-line detection using appropriate flow cells. By selective removal of the solvent matrix, the absorption problem might be solved, enabling the acquisition of the full IR spectrum of the analyte. However, nonvolatile solvents such as water require sophisticated elimination systems and the use of microbore columns. Ultrasonic treatment,<sup>3</sup> particle beam interfacing,<sup>4</sup> and concentric flow nebulization<sup>5</sup> are a few examples of the elimination strategies that have been successfully coupled to reversed-phase HPLC. For the other approach, on-line detection, the flow cell must be able to handle high liquid flow rates and nonvolatile eluent constituents such as salts and buffers. To limit the solvent absorption, the optical path length must also be reduced, which in turn reduces sensitivity. Despite the reduction in optical path length, some spectral regions are still difficult to access, especially when working with aqueous solutions, due to the extremely strong water absorption (particularly the bending vibration of water around 1640  $\text{cm}^{-1}$ ). Nevertheless, FT-IR has been successfully coupled to HPLC by use of a 25- $\mu\text{m}$  CaF<sub>2</sub> flow cell for the on-line detection of carbohydrates, alcohols, and organic acids in wines<sup>6</sup> and sugars in nonalcoholic beverages.<sup>7</sup>

Capillary Electrophoresis (CE) is an electrically driven process primarily used to separate ionized and partially ionized species in aqueous solutions, although nonaqueous solvents have also been used.<sup>8</sup> Frequently cited advantages of CE include its high efficiency (theoretical plate numbers are often over half a million), the rapidity of the analysis that can usually be achieved, and the extremely small sample volumes required. However, detection of analytes in CE offers a significant challenge because of the narrow bore of the capillary (typically between 25 and 75  $\mu\text{m}$ ). The most common mode of detection is UV absorption, but other types of

\* Corresponding author. Tel.: +4315880115140. Fax: +4315880115199. E-mail: blendl@mail.zserv.tuwien.ac.at.

<sup>†</sup> Stockholm University.

<sup>‡</sup> Institute of Chemical Technologies and Analytics, Vienna University of Technology.

<sup>§</sup> Industrial Electronics and Material Science, Vienna University of Technology.

(1) Griffiths, P. R.; Pentoney, S. L., Jr.; Giorgetti, A.; Shafer, K. H. *Anal. Chem.* **1986**, *58*, 1349A–1366A.

(2) Fujimoto, C.; Jinno, K. *Anal. Chem.* **1992**, *64*, 476A–481A.

(3) Castles M. A.; Azarraga L. V.; Carreira L. A. *Appl. Spectrosc.* **1986**, *40*, 673–680.

(4) Turula, V. E.; de Haseth, J. A. *Appl. Spectrosc.* **1994**, *48*, 1255–1264.

(5) Lange, A. J.; Griffiths P. R.; Fraser, D. J. *J. Anal. Chem.* **1991**, *63*, 782–787.

(6) Vonach, R.; Lendl, B.; Kellner, R. *J. Chromatogr. A* **1998**, *824*, 159–167.

(7) Vonach, R.; Lendl, B.; Kellner, R. *Anal. Chem.* **1997**, *69*, 4286–4290.

(8) Riekkola, M.-J.; Jussila, M.; Porras, S. P.; Valk  , I. E. *J. Chromatogr. A* **2000**, *892*, 155–170.

detectors that have also been successfully coupled to CE include laser-induced fluorescence, mass spectrometry, electrochemical, conductivity, and Raman scatter monitoring instruments.<sup>9–13</sup> Although CE requires only nanoliter volumes of sample, it is not a trace analysis technique. Relatively concentrated analyte solutions or preconcentration methods are often needed. To improve sensitivity and reproducibility, methods for on-capillary sample preconcentration (stacking) can be used, and reproducible injections can be provided by hyphenation of CE to FIA.<sup>14–17</sup>

In 1998, de Haseth et al. presented a preliminary study of CE with off-line FT-IR detection.<sup>18</sup> A metal nebulizer interface was designed, and the eluate from the CE was deposited on a ZnSe window. The sample deposits were subsequently measured with a FT-IR microscope. Due to the difficulties involved with obtaining complete elimination of nonvolatile solvents, the separation buffer had to be volatile. Spectra could be obtained from a 50-ng injected sample.

In this study, a method was developed for coupling the on-line, universal, and molecule-specific detection offered by FT-IR with CE. Since silica capillaries absorb IR radiation almost totally, a completely new flow cell has been developed. The successful on-line hyphenation of CE and FT-IR offers obvious advantages, such as the possibility of using any kind of buffer as well as real-time signal output. Furthermore, the constant measurement conditions in the flow cell allow easy subtraction of the “pure” buffer IR absorption spectrum from the recorded spectra.

## EXPERIMENTAL SECTION

**Preparation of the Flow Cell.** The procedure developed for making the CE-FT-IR cells allowed for the simultaneous production of ~40 cells. Two CaF<sub>2</sub> disks (30 mm in diameter and 1 mm thick) were used as starting material (Figure 1a). On one of these disks, a 200-nm-thick titanium layer was deposited by evaporation and patterned by a conventional liftoff technique. The titanium acted as an optical aperture preventing strong IR absorption by the polymer layers surrounding the flow channel. The titanium layer was isolated to prevent electrical contact with the CE separation buffer. The flow channel was formed by two streaks (100  $\mu$ m wide and ~7  $\mu$ m thick) of epoxy-based photoresist SU-8 (Microchem Corp., Newton, MA) on each CaF<sub>2</sub> disk, producing a channel 150  $\mu$ m wide and 15  $\mu$ m thick. Both CaF<sub>2</sub> disks were spin-coated with SU-8 and soft-baked (90 °C, 30 min.). After UV exposure (30 s) using a SUSS MJB3 mask aligner (Suss Microtech, Munich, Germany) and an appropriate photomask, the photoresist was postexposure-baked (95 °C, 10 min) and developed with propylene glycol monomethyl ether acetate (PGMEA). The unexposed (and therefore not cross-linked) area was dis-

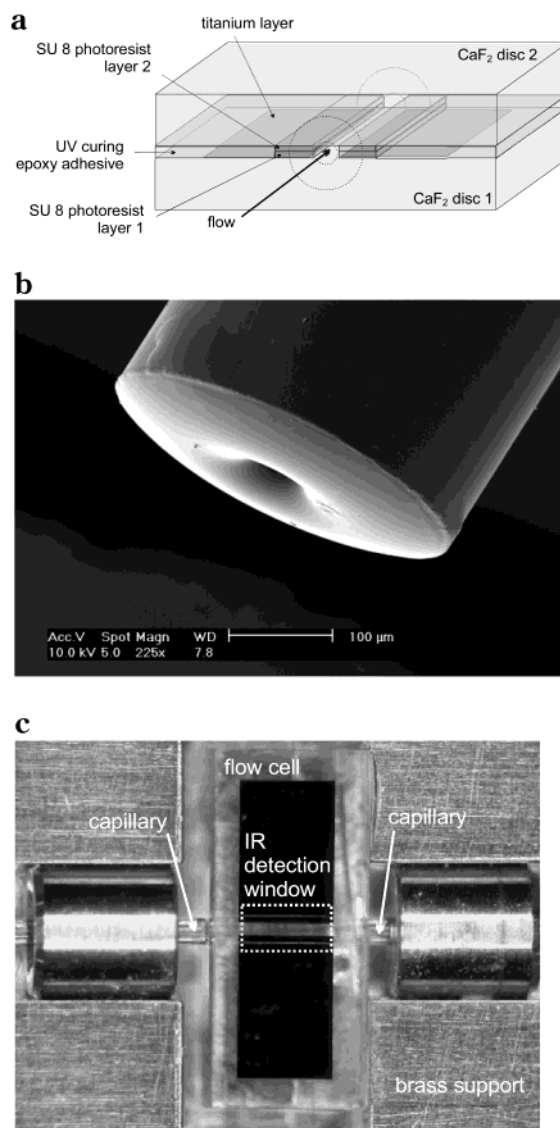


Figure 1. (a) Schematic view of the CE-FT-IR cell (with scaling altered to show details of key features). (b) SEM micrograph showing the capillary O-ring. (c) Microscopic view of the CE-FT-IR cell, with connected capillaries, housed in its supporting block.

solved during this process. The two disks, one with and one without the metal structure, were superimposed and compressed during the hard-bake process (200 °C, 1 h). Consequently, the two disks were bonded by the SU-8 structure since the high temperature induces a complete cross-linking of the SU-8. This hard bake was necessary to develop the full mechanical strength and chemical resistance of the SU-8. Finally, the areas outside the SU-8 streaks were filled with UV-curing epoxy adhesive (Delo Katiobond 4653, Delo, Landsberg, Germany) and the wafer (two disks bonded together) was cut with a dicing saw. In this manner, 40 cells could be manufactured from one wafer. The surfaces where the capillaries are coupled (the inlet and outlet of the flow channel) of each cell were polished with a 3- $\mu$ m lapping film to ensure a tight connection between the capillaries and the cell. To couple the capillaries to the flow cell, a small drop of UV-curing epoxy adhesive was placed on one end of the capillaries while a gentle stream of air was passed through them. In this way, a small elastic O-ring was formed that enabled a tight connection (Figure

- (9) Foret, F.; Krivankova, L.; Bocek, P. *Capillary zone electrophoresis*; VCH: Weinheim, 1993.
- (10) Khaleli, M. G. *High performance capillary electrophoresis: Theory, techniques and applications*; Wiley Inc.: New York, 1998.
- (11) von Brocke, A.; Nicholson, G.; Bayer, E. *Electrophoresis* **2001**, *22*, 1251–1266.
- (12) Swinney, K.; Bornhop, D. J. *Electrophoresis* **2000**, *21*, 1239–1250.
- (13) Kuyper, C.; Milofsky, R. *Trends Anal. Chem.* **2001**, *20*, 232–240.
- (14) Kuban, P.; Karlberg, B. *Anal. Chem.* **1997**, *69*, 1169–1173.
- (15) Kuban, P.; Karlberg, B. *Trends Anal. Chem.* **1998**, *17*, 34–41.
- (16) Kuban, P.; Berg, M.; García, C.; Karlberg, B. *J. Chromatogr., A* **2001**, *912*, 163–170.
- (17) Fang, Z.-L.; Fang, Q. *Fresenius' J. Anal. Chem.* **2001**, *370*, 978–983.
- (18) He, L.-T.; de Haseth, J. A. *AIP Conf. Proc.* **1998**, *430*, 407 (Fourier Transform Spectroscopy).

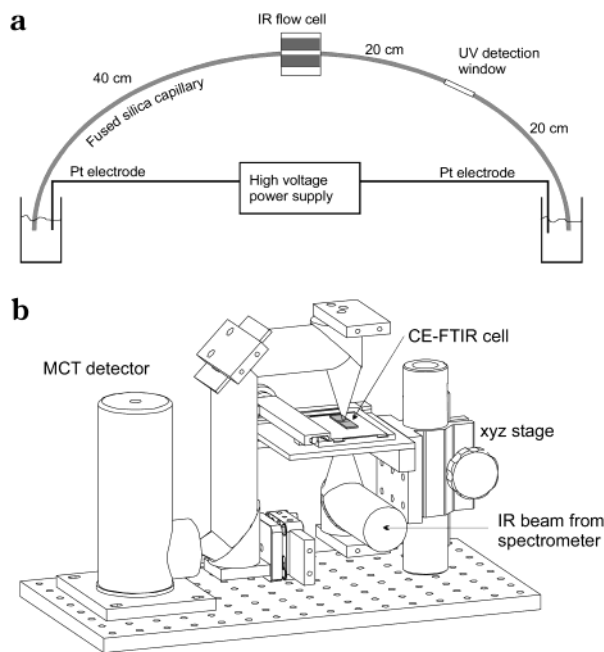


Figure 2. (a) Schematic diagram of the experimental setup. (b) Optical setup: the IR beam from the spectrometer is focused on the flow channel of the CE-FT-IR cell by means of a parabolic mirror and then on a highly sensitive MCT detector.

1b). The flow cell was then put into a custom-built supporting block allowing fine adjustment of the cell and the capillary (Figure 1c). The cell was placed in a groove in the support, and the capillaries were coupled to the flow channel of the cell through bolts fixed adjacent to it. This arrangement allowed for easy replacement of both the cell and the capillaries.

**Experimental Setup.** A schematic view of the experimental setup including the capillary electrophoresis system, the FT-IR spectrometer, and the UV detector is depicted in Figure 2a.

**Capillary Electrophoresis System.** The CE system, which was built in-house, consisted of a high-voltage power supply (Brandenburg, Thornton Heath, U.K.), two platinum electrodes, and untreated fused-silica capillaries (i.d. 50  $\mu\text{m}$ , o.d. 375  $\mu\text{m}$ , Polymicro Technologies, Phoenix, AZ). The separation voltage applied (at the injection end of the capillary) was +20 kV, resulting in a current of 22  $\mu\text{A}$  measured over a 100-k $\Omega$  resistance. New capillaries were preconditioned with 0.1 M NaOH, distilled water, and buffer prior to use. The capillary surface was refreshed at start-up each day by the use of 0.1 M NaOH and buffer. No further cleaning was necessary in order to maintain capillary performance. The total capillary length was 80 cm, and the length from the injection point to the IR cell was 40 cm, with an additional 20 cm to the UV cell (Figure 2a). Hydrodynamic injection of the samples was performed by lifting the injection side of the capillary 27 cm for 20 s, resulting in sample injection volumes of 10 nL.

**FT-IR Spectrometer.** A Bruker Equinox 55 FT-IR spectrometer (Bruker Optik GmbH) was used throughout all the experiments. To enable the IR beam to be focused correctly, the IR window of the capillary was placed in an external optical focusing unit, constructed in-house,<sup>19</sup> in a Perspex unit purged with dry air. The IR beam from an external optical port of the spectrometer was focused on the cell by means of an off-axis parabolic mirror and then on a highly sensitive mercury cadmium telluride (MCT)

detector (Figure 2b). The scanner of the spectrometer was operated at a HeNe laser modulation frequency of 150 kHz. Fifty scans were coadded for each spectrum with a spectral resolution of 16  $\text{cm}^{-1}$  (background spectra 500 coadditions). A low-pass filter with a 5% cut-on at 1900  $\text{cm}^{-1}$  was inserted in the IR beam to increase the light throughput in the spectral region of interest (1800–900  $\text{cm}^{-1}$ ).

Reference measurements of the analytes were obtained by attenuated total reflection (ATR), using a diamond ATR cell (SensIR, Danbury, CT) with a circular surface of 3 mm and nine internal reflections. For these measurements, the scanner velocity (HeNe laser modulation frequency) was 100 kHz and 100 scans were coadded for each spectrum.

**UV Detector.** A CV<sup>4</sup> UV–visible detector (Isco, Lincoln, NE) set at 254 nm and an ELDS Pro 1.0 laboratory data system (Chromatography Data systems, Kungshög, Sweden) were used to register the UV electropherograms. The UV detection window was made by burning away a small piece of the surrounding polyamide coating on the capillary.

**Chemicals.** Adenosine, guanosine, adenosine-5'-monophosphate (AMP), and Borax were all of analytical grade (Fluka, Buchs, Switzerland). Stock solutions of 8 mM adenosine, 8 mM AMP, and 3.2 mM guanosine were made by dissolving the respective analyte in 0.2- $\mu\text{m}$  filtered HPLC water (Fluka). A 15 mM Borax buffer, adjusted to pH 10 with NaOH, was employed as carrier electrolyte. Before introduction into the system, all solutions were degassed for 15 min in an ultrasonic bath.

## RESULTS AND DISCUSSION

**CE-FT-IR–UV Recordings.** Figure 3a shows a typical electropherogram illustrating the separation of adenosine (6 mM), guanosine (2.4 mM), and AMP (6 mM) recorded with the conventional UV detector placed immediately after the IR cell. Due to deliberately selected differences in conductivity between the analytes and the electrolyte, three different peak shapes can be distinguished: a leading peak for adenosine, a Gaussian peak for guanosine, and a tailing peak for AMP. It should be stated here that the separation under these conditions has not been completely optimized, since this was not the purpose of the presented work. However, it is of interest to elucidate how the difference in the peak shape, as shown in the UV electropherograms, influences the detection with FT-IR spectroscopy. Panels b–d of Figure 3 show 3-D stack plots of FT-IR spectra recorded during the same run. The peak shapes represented in the UV electropherogram are clearly confirmed by the recorded FT-IR spectra. The stack for adenosine shows a slow increase and abrupt decrease in the intensity of the spectrum, with the strongest feature located between 1000 and 1200  $\text{cm}^{-1}$ , mainly due to the C–O stretch vibration of the carbohydrate (Figure 3b). For the short Gaussian CE peak of guanosine, only three spectra can be recorded (Figure 3c). When AMP passes the FT-IR cell, a sudden increase in the signal from the strong phosphate band around 1100  $\text{cm}^{-1}$  is noted (Figure 3d), followed by a slow decrease in accordance with the UV electropherogram.

The signal of the sample bulk was clearly detected as a negative IR spectrum of the buffer (Borax). In this context, it is

(19) Hinsmann, P.; Haberkorn, M.; Frank, J.; Svasek, P.; Harasek, M.; Lendl, B. *Appl. Spectrosc.* **2001**, *55*, 241–251.



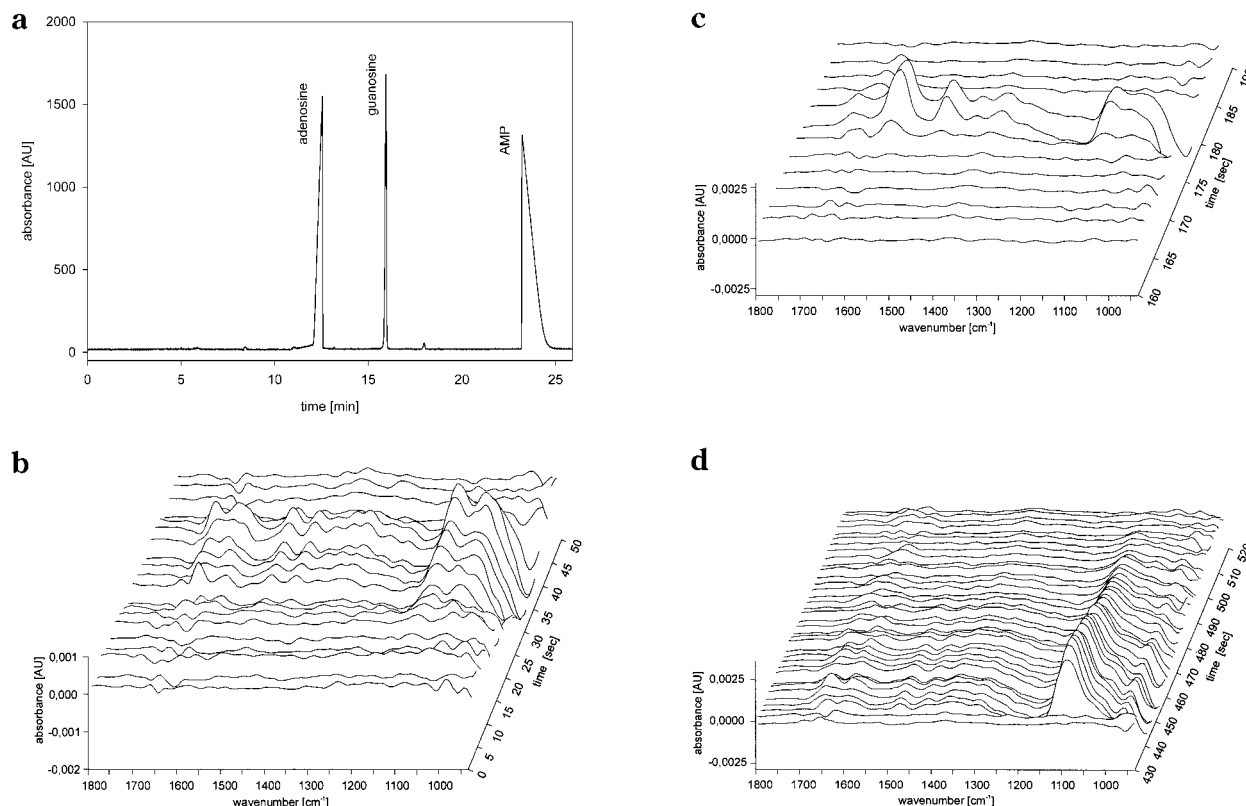


Figure 3. (a) Electropherogram with conventional UV detection at 254 nm showing a separation of adenosine, guanosine, and AMP. CE conditions: 15 mM Borax buffer at pH 10, hydrodynamic injection 20 s at 27 cm height, 250 V/cm, and 60 cm to UV detection. (b–d) 3-D stack plots of infrared spectra from a separation of adenosine (b), guanosine (c), and AMP (d).

also interesting to note that the background spectrum of the buffer changed after the sample bulk had passed the cell. Therefore, a new background spectrum had to be recorded after its passage.

The FT-IR spectra recorded at the CE peak maximums were compared to those measured separately for each of the three analytes in a conventional ATR cell. The comparative results, depicted in Figure 4, clearly show the similarity of the spectral features obtained with the two techniques. The intensity of these spectra cannot be directly compared due to the difference in the optical path length. However, it is interesting to compare the relative intensities obtained for the three analytes: for both adenosine and AMP (Figure 4a and c), the spectra taken with the ATR show higher absorption signals than those obtained in the CE-FT-IR cell, but the reverse is observed for guanosine (Figure 4b). This is because the separation system is optimized for guanosine, yielding a narrow, Gaussian peak.

To investigate whether (and how) peak shapes, peak heights, and retention times were influenced by incorporation of the new IR flow cell, UV recordings were obtained with and without the IR flow cell connected in series before the UV detector. Capillaries from the same batch were used, and in both cases, the total length of the separation capillary was 80 cm while the distance to the UV detector was 60 cm. In the experiment including the IR flow cell, it was placed as close to the UV detector as possible (20 cm). The recorded guanosine peaks are shown in Figure 5. As can be seen, hardly any zone broadening occurs due to the incorporation of the IR. Furthermore, changes in both the retention time and the peak height were within the variation generally observed in the separation, despite the fact that the cross section of the IR

cell ( $150 \times 15 \mu\text{m}$ ) differed considerably from the inner diameter of the capillary. The results clearly demonstrate that the IR cell we developed does not adversely affect the performance of the CE separation and thus allows tandem detection.

**Variation of FT-IR Parameters.** The time required for recording spectra in FT-IR spectroscopy is governed by the speed at which the optical path difference is generated in the interferometer, by the desired number of coadditions of scans per spectrum, and by the spectral resolution. Under optimized separation conditions, CE peaks pass through the flow cell in a few seconds, like guanosine in the system investigated in this work. In such cases, the time for recording IR data is limited. Care has to be taken to accumulate a sufficiently large number of scans to achieve a high signal-to-noise ratio for each spectrum and to maintain a high temporal resolution of subsequent FT-IR spectra. In our experiments, we reduced the spectral resolution to  $16 \text{ cm}^{-1}$ , which is rather low when compared to standard measurements in liquid phase, but still sufficient to resolve the spectral characteristics of our analytes. A parameter that was studied in more detail was the scan velocity, expressed as the Fourier frequency of the HeNe laser used to determine the optical path difference. The scanner velocity was varied between 80 and 200 kHz, and 50 scans were coadded for each spectrum. Under these conditions, the time required for recording one spectrum was 3.5 s at a scanner velocity of 80 kHz and 2.2 s at a scanner velocity of 200 kHz. The small difference in time required for recording a spectrum under these extremes is due to the considerable amount of time lost between consecutive scans, because the direction of the mirror's movement must be reversed.

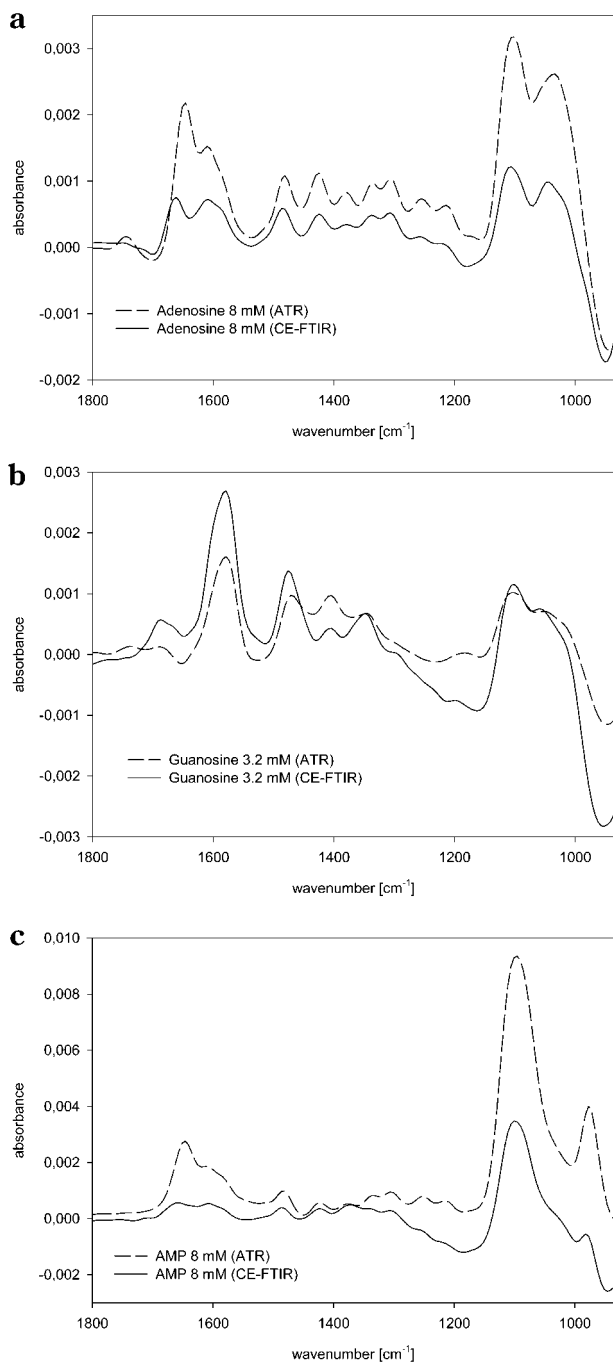


Figure 4. Comparison of the spectra obtained from adenosine (a), guanosine (b), and AMP (c) with an ATR and the CE-FT-IR cell during a separation.

Consequently, no clear optimum scan speed could be identified. Therefore, for further measurements, the scanner velocity was set to 150 kHz. Coaddition of 50 scans/spectrum still allowed three spectra to be recorded during the residence time of the sharpest CE peak in the detector flow cell. It should be mentioned here that under these experimental conditions an increase in temporal resolution is only possible at the expense of the signal-to-noise ratio of the spectra. In this context, a new interferometer design based on a rotating mirror to introduce the optical path difference shows great promise,<sup>20</sup> as it allows the number of scans recorded per second to be increased by  $\sim 1$  order of magnitude. This instrumental development therefore has the potential to further

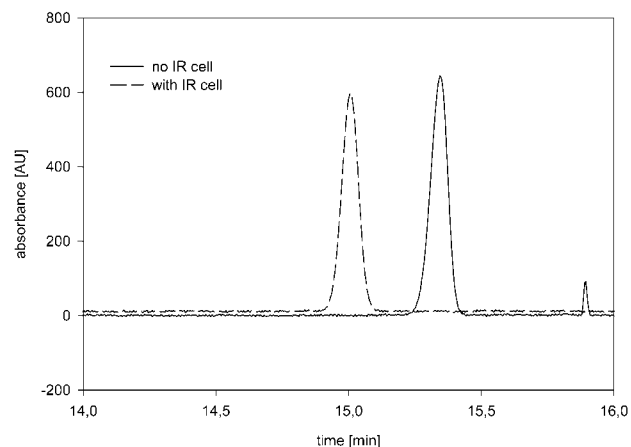


Figure 5. Comparison of the guanosine peak from a separation with and without incorporation of the CE-FT-IR cell.

Table 1: FT-IR Calibration Results<sup>a</sup>

	intercept	slope	$r^2$	$S_y$	$S_{x0}$	LOD (mM)	LOD (pg)
adenosine	0.0952	0.0788	0.998	0.011	0.140	0.42	1150
guanosine	0.0396	0.0913	0.994	0.009	0.094	0.28	800
AMP	-0.0646	0.7075	0.999	0.061	0.087	0.26	900

<sup>a</sup>  $r^2$ , regression coefficient;  $S_y$ , standard deviation of residuals;  $S_{x0}$ , standard deviation of the method; LOD, limit of detection.

increase the number of scans and thus the signal-to-noise ratio of the spectra recorded from single CE peaks.

**Calibration and Limit of Detection Studies.** To obtain figures of merit for the calibration and to determine the limit of detection of the presented method, the concentration of the injected sample was varied between 8 and 0.8 mM for adenosine (2.14–0.21 g/L) and AMP (2.78–0.28 g/L) and between 3.2 and 0.64 mM (0.91–0.18 g/L) for guanosine.

The calibration was done by calculating the area below the band between 1114 and 1077  $\text{cm}^{-1}$  with respect to a baseline defined by two baseline points, at 1764 and 1188  $\text{cm}^{-1}$ . The peaks in the resulting FT-IR electropherograms were then integrated by calculating the area under them. This integration method could be applied to all three analytes, since all of them exhibit a strong spectral feature in this range (C–O stretch vibration for adenosine and guanosine and the phosphate band for AMP). The lowest limit of detection (3 S/N), 800 pg, was achieved for guanosine. The calibration results are summarized in Table 1. Triplicate injections were done to measure the reproducibility of the retention time and peak area.

## CONCLUSIONS

The study detailed in this paper describes, to the authors' knowledge, the first successful on-line coupling of a Fourier transform infrared detection system with capillary electrophoresis. The IR detection limits achievable with this system are remarkably low, partly due to the stacking that occurs in the sample plug in the capillary. Detection limits as low as 800 pg were recorded for aqueous solutions of guanosine. The inherent potential of IR

(20) Griffiths, P. R.; Hirsch, B. L.; Manning, C. J. *Vib. Spectrosc.* **1999**, *19*, 165–176.

detection lies in its excellent ability to identify analytes, which is useful in applications such as pharmaceutical analyses, where not only quantification but also identification of analytes is extremely important. In this respect, FT-IR detection offers a unique spectrum for each separated analyte. The designed flow cell enables nondestructive, real-time detection and the option to add further detectors for simultaneous use in the flow system.

Future work will focus on diversifying the CE separation techniques and replacement of the FT-IR interferometer with more powerful mid-IR light sources, such as quantum cascade lasers. The powerful emission characteristics of such light sources would allow both the sensitivity and the exploitable optical path length to be increased, giving access to spectral regions where solvent

interference is usually too high to allow acquisition of useful information about the analyte under investigation.<sup>21</sup>

#### ACKNOWLEDGMENT

The European Union Marie Curie Training Site on Advanced and Applied Vibrational Spectroscopy (Contract HPMT-CT-2000-00059), the Austrian Science Fund (Project FWF 13350), and FOSS Tecator are gratefully acknowledged for financial support.

Received for review February 19, 2002. Accepted May 7, 2002.

AC025590T

---

(21) Kölhed, M.; Pustugov, V.; Mizaikoff, B.; Haberkorn, M.; Frank, J.; Karlberg, B.; Lendl, B. *Vib. Spectrosc.* **2002**, in press.